

Predicted disconnectome associated with progressive periventricular white matter ischemia

Zhengjun Li^{a,d,e,f}, Sudipto Dolui^{b,d,e,f}, Mohamad Habes^{a,b,d,e,f,h}, Danielle S. Bassett^{a,c,d,e,f,g}, David Wolk^{a,d,e,f}, John A. Detre^{a,b,d,e,f,*}

^a Departments of Neurology, University of Pennsylvania, 3W Gates Pavilion, 3400 Spruce Street, Philadelphia, PA 19104, USA

^b Radiology, USA

^c Psychiatry, USA

^d Bioengineering, USA

^e Physics & Astronomy, USA

^f Electrical and Systems Engineering, University of Pennsylvania Perelman School of Medicine, USA

^g The Santa Fe Institute, USA

^h Biggs institute neuroimaging core (BINC), Glenn Biggs Institute for Alzheimer's and Neurodegenerative Diseases, University of Texas Health Sciences Center, USA

ARTICLE INFO

Keywords:

Periventricular white matter (PVWM)

Small vessel ischemic disease

DTI

fMRI

Structural connectivity

Functional connectivity

Cerebral blood flow (CBF)

ABSTRACT

We used a virtual lesion DTI fiber tracking approach with healthy subject DTI data and simulated periventricular white matter (PVWM) lesion masks to predict the sequence of connectivity changes associated with progressive PVWM ischemia. We found that the optic radiations, inferior fronto-occipital fasciculus, inferior longitudinal fasciculus, corpus callosum, temporopontine tract and fornix were affected in early simulated ischemic injury, and that the connectivity of subcortical, cerebellar, and visual regions were significantly disrupted with increasing simulated lesion severity. The results of this study provide insights into the spatial-temporal changes of the brain structural connectome under progressive PVWM ischemia. The virtual lesion approach provides a meaningful proxy to the spatial-temporal changes of the brain's structural connectome and can be used to further characterize the cognitive sequelae of progressive PVWM ischemia in both normal aging and dementia.

Introduction

White matter (WM) lesions, typically detected as hyperintensities on T2-weighted fluid attenuated inversion recovery (FLAIR) sequence in magnetic resonance imaging (MRI), are highly prevalent in older adults [1], including asymptomatic individuals [2]. White matter hyperintensities (WMH) in aging populations appear first and more frequently in the periventricular white matter (PVWM) [3] as variable size caps on the frontal and occipital horns, and as thin rims along the walls of the lateral ventricles. With increasing severity PVWM lesions may become confluent with lesions that occur in the deep white matter (DWM). PVWM lesions are more ubiquitous than DWM lesions [4,5], and may be specifically associated with cognitive and functional decline [6–8]. PVWM lesions, along with DWM lesions, lacunar infarcts, and microhemorrhages, underlie the syndrome of subcortical vascular cognitive impairment and also contribute to dementia accompanying Alzheimer's disease [1,9–12].

PVWM lesions are thought to result primarily from chronic progressive ischemic microangiopathy [1], but are not specific for this mechanism. However, the mechanisms by which PVWM lesions selectively alter cognitive function remain uncertain, in part because these lesions are typically seen with comorbid brain pathologies. There is also mounting evidence that both functional and microstructural changes in the PVWM may precede the development of overt WMH based on T2-weighted MRI [13–15]. Chronic hypoperfusion observed in the PVWM [7,16,17] can alter molecular pathways, disrupting paranodal and axon-glia integrity and resulting in white matter disintegration [18] and impaired signal conduction along affected pathways. Accordingly, it is possible that WM lesions based on T2-weighted MRI alone may underestimate the extent to which WM pathways are affected by progressive PVWM lesions.

* Corresponding author at: Departments of Neurology, University of Pennsylvania, 3W Gates Pavilion, 3400 Spruce Street, Philadelphia, PA 19104, USA.

E-mail address: detre@penmedicine.upenn.edu (J.A. Detre).

<https://doi.org/10.1016/j.cccb.2021.100022>

Received 15 December 2020; Received in revised form 28 June 2021; Accepted 29 June 2021

Available online 1 July 2021

2666-2450/© 2021 The Authors.

Published by Elsevier B.V. This is an open access article under the CC BY-NC-ND license

(<http://creativecommons.org/licenses/by-nc-nd/4.0/>).

Disconnection as a mechanism of neurological deficits due to white matter lesions

White matter lesions classically cause disconnection syndromes by interrupting communication between the brain regions that they connect, such as hemiparesis with lesions affecting the corticospinal tracts. The distributed network properties of the brain can now be studied noninvasively using magnetic resonance imaging (MRI) methods including diffusion tractography (DTI) to infer structural connectivity in WM or using correlated fluctuations in blood oxygen level dependent (BOLD) resting-state fMRI to study functional connectivity between gray matter regions [19]. The term “connectome” refers to the connectivity matrix between gray matter nodes. The disruptions to normal connectivity matrix is termed the “disconnectome” [20].

Prior research using DTI data acquired in patients with small vessel disease has demonstrated alterations in structural network properties that correlate with cognitive decline [21–24], and a recent study performed in a large middle aged cohort in whom both structural MRI, DTI, and cognitive testing were available demonstrated that the structural disconnectome due to WMH was a stronger prediction of cognition that was the structural connectome [20].

Given the ubiquity of PVWM hyperintensities even in healthy aging, identifying the structural connectivity affected is of interest in further characterizing the mechanisms and progression of age-associated cognitive decline. Although early stage PVWM hyperintensities are small, their impact on structural connectivity may be relatively widespread because multiple white matter tracts cross as they skirt around the ventricles [25].

Use of a virtual lesion approach to predict the disconnectome due to PVWM lesions

Two main factors make it challenging to isolate the impact of PVWM lesions on structural connectivity in the adult human brain. Firstly, lesions can alter the diffusion properties of WM and disrupt computerized tract-tracing algorithms, resulting in abnormal structural connectomes [26–30]. Secondly, while the PVWM shows by far the highest WM lesion frequency across cohorts, individual subjects with PVWM lesions typically also have lesions elsewhere in the WM.

To circumvent these limitations, in this study we used a virtual lesion method [31] with simulated PVWM ischemia inserted as regions of avoidance (ROA) to conduct DTI fiber tracking using young healthy subjects’ diffusion data from the Human Connectome Project (HCP). Use of a virtual lesion approach with ROA avoids the problems associated with performing tractography using patient DTI data containing lesions. To contrast with “direct” connectivity mapping using DTI data from lesioned patients’ own scans, this virtual lesion approach has also been termed “indirect” mapping [32].

Secondly, to simulate the effects of PVWM ischemia, we built upon our recent work demonstrating that the distribution of PVWM lesions corresponds to the distribution of white matter perfusion, which is lowest in the periventricular region [33]. In our prior study, we characterized spatial variations in white matter CBF using a group CBF map obtained from a large cohort of middle-aged adults from the Coronary Artery Risk Development in Young Adults (CARDIA) study. We observed a gradient of reduced perfusion around the ventricles the morphology of which was spatially consistent with known patterns of increasing WMH frequency [3,5].

A benefit of using CBF-derived ischemic lesion masks is that this approach naturally results in a periventricular distribution based on the CBF gradient [33], without requiring arbitrary anatomical boundaries to define the periventricular zone. Furthermore, prior research has demonstrated that white matter hyperintensities have a “penumbra” [13–15,34–36], with lesions expanding into adjacent voxels over time. Since periventricular CBF varies smoothly in our group CBF map from CARDIA data, this type of progression is also simulated in our approach

of using increasing CBF thresholds. Finally, because our CBF-based ischemic lesion masks are derived from data acquired in middle aged subjects, coregistration errors between the lesion masks and HCP DTI data acquired from young adults are reduced.

In summary, the overall aim of this study was to evaluate the use of indirect tractography with CBF-defined ROA as a means of characterizing the widespread partial connectivity changes likely to be associated with progressive PVWM ischemia.

Methods

Human subject data

We used high resolution DTI data from 30 healthy young subjects (15 Female, 5 subjects in age range 22–25 yrs, 17 subjects in age range 26–30 yrs, 8 subjects in age range 31–35 yrs) from the publicly available Human Connectome Project (HCP) S900 release [37]. The subjects’ MRI images were acquired using protocols approved by the Institutional Review Board (IRB) of Washington University in Saint Louis.

Diffusion MRI data from the HCP young subjects were acquired $1.25 \times 1.25 \times 1.25 \text{ mm}^3$ for connectivity mapping using a 3T Siemens scanner customized for the Human Connectome Project (Siemens Healthineers, Erlangen, Germany). The parameters used were as follows: TR/TE = 5520/89.5 ms, 268×144 matrix on a $210 \times 180 \text{ mm}$ FOV, 111 slices. A total of 90 diffusion weighting directions of 3 shells of $b = 1000, 2000, \text{ and } 3000 \text{ s/mm}^2$ in addition to six $b = 0$ images were acquired [38].

To validate the notion that an indirect virtual lesion approach based on CBF-derived ischemic lesion masks can be used to infer the effects of PVWM ischemia on structural connectivity, we also examined structure-function relationships in multimodal MRI data acquired in an older cohort of 46 cognitively normal and amyloid-negative older subjects (31 female, age = 72.30 ± 6.81 years) that included FLAIR images used to segment WM hyperintensities (WMH), resting-state fMRI data used to compare predicted changes in structural connectivity to changes in functional connectivity, and DTI data used to compare native DTI tractography to indirect tractography using HCP young subjects’ data with and without the addition of virtual lesions. The 3T Siemens Prisma (Siemens Healthineers, Erlangen, Germany) scanning protocol in this older cohort included a 0.8 mm isotropic T1-MPRAGE structural MRI scan (TR/TE/TI = 2400/2.24/1060 ms); an 8 min multiband BOLD-EPI scan: TR/TE = 720/37 ms, flip angle 52° , acquisition matrix = 104×104 on a $208 \times 208 \text{ mm}$ FOV, 72 slices with slice thickness = 2 mm, and 420 time points; a 3D 1 mm isotropic FLAIR scan (TR/TE/TI = 6000/289/2200 ms), acquisition matrix = $256 \times 220, 160$ slices; a dual-echo field map scan for field inhomogeneity correction; a diffusion weighted image scan: $1.5 \times 1.5 \times 1.5 \text{ mm}^3$ resolution (TR/TE = 3027/82.8 ms), 140×140 matrix in a $120 \text{ mm} \times 210 \text{ mm}$ FOV using multi-shell DTI consisting of three b-values (300, 800, 2000 s/mm^2) acquired along 15, 30, 64 uniformly distributed directions, respectively, with 9 additional $b = 0$ images acquired. The majority of these studies are described in the Supplement.

White matter hyperintensities in relation to CBF

To demonstrate the homology between the distribution of white matter hyperintensities (WMH) and periventricular CBF, we segmented WMH from the older cohort using the automated lesion growth algorithm (LGA) [39] implemented in the lesion segmentation tool (LST) software (version 2.0.15, <https://www.applied-statistics.de/lst.html>) for SPM 12. The LGA segments the T1 structural scan into gray matter, white matter and cerebrospinal fluid (CSF) maps and compares them with the FLAIR intensities to calculate the lesion belief map. The lesion belief map was initially thresholded with the recommended value (cutoff threshold of belief value $\kappa = 0.3$) [39] and subsequently grown along voxels with hyper-intensity in the FLAIR image to generate the

lesion map. All subjects' lesion maps were verified by visual inspection for quality and then warped to the MNI space.

Gray matter nodes used for connectivity analysis

To test the effects of white matter ischemia on structural and functional connectivity, we analyzed the network connectivity of the whole brain using the 333 cortex parcellation recently published by Gordon et al. [40], combined with 40 subcortical and cerebellar ROIs from the AAL atlas [41] for a total of 373 nodes. The atlas was used for DTI fiber streamline tracking in MNI space using DSI Studio [42], and for extracting the mean time series of resting-state fMRI signals in MNI space as explained in the next sections.

Structural connectivity analysis

Structural connectivity was obtained using DSI Studio [42]. First the diffusion data were reconstructed using the q-space diffeomorphic reconstruction (QSDR) to calculate the spin orientation distribution of diffusing water in a common stereotaxic space. Then 10^7 seed points were used for whole brain deterministic streamline fiber tracking to generate whole brain WM tracks. The number of tracts connecting each pair of parcellated ROIs were normalized by dividing the sum of the volumes of the paired ROIs [43] to construct the weighted structural connectivity network matrix of the given parcellation. For the network analysis, a group representative structural connectivity matrix mask was created by retaining edges with the 10% strongest consistency estimates [44], excluding edges between physically nearby ROIs (<20 mm) [45].

Predicted disconnectome due to progressive PVWM ischemia

To simulate progressive PVWM ischemic lesions, we created a series of masks using the white matter CBF distribution map from a previous study of a large cohort of middle-aged subjects [33] and by masking that map with thresholds from 8 to 20 ml/100 g/min in steps of 1 ml/100 g/min. To mimic the age-dependent evolution of the PVWM lesion disconnectome, these CBF-derived ischemic lesion maps were then used

as ROA for indirect structural connectivity mapping in the 30 HCP young subjects' DTI data in the HCP S900 release. At each step, we used the mask as a ROA for structural connectivity tracking on $N = 30$ DTI scans from young healthy subjects to selectively identify the WM pathways most likely to be affected by progressive PVWM ischemia. In the virtual lesion approach, any streamlines calculated to pass through the ROA are deleted from the resulting connectome. The connectivity matrices with ROA and the connectivity matrices without ROA were then compared to examine the vulnerability of the structural connectivity pattern to the synthetic lesions. This processing pipeline is illustrated in Fig. 1. Note that while CBF map thresholds are provided in quantitative CBF units of ml/100 g/min, as described in [33], white matter CBF was likely underestimated using the arterial spin labeled perfusion MRI as implemented in the CARDIA study.

To test the vulnerability of anatomical WM tracts to the progressive PVWM ischemia simulated using thresholded CBF masks, we also utilized the population-averaged white matter tractography atlas ("HCP842") published by DSI Studio (version 2019) which contains 80 WM tracts labeled by neuroanatomists to conform to previous neuroanatomical knowledge [46]. We conducted streamline tractography (10^7 seed points) on the 30 HCP young subjects to extract the 80 pathways [46,47] and examined the average percentage of the affected fibers of these pathways in the presence of simulated ischemic PVWM ischemic lesions created with stepwise CBF thresholds. The affected tracts include fibers passing through the regions of avoidance. The percentage of affected fibers was calculated as the ratio of the number of affected fibers for a given lesion to the number of fibers without the presence of any lesion.

Statistical methods

The Structural connectivity of the 30 HCP young subjects were produced for two conditions: (1) using the (simulated) lesion mask as region of avoidance; (2) no region of avoidance. A paired-T test was conducted for each edge in the 10% strongest consistency estimates mask. Bonferroni correction was used to control for multiple comparison error. Edges with $p < 0.05$ after Bonferroni correction were collected as the significant lesion based DTI disconnectome.

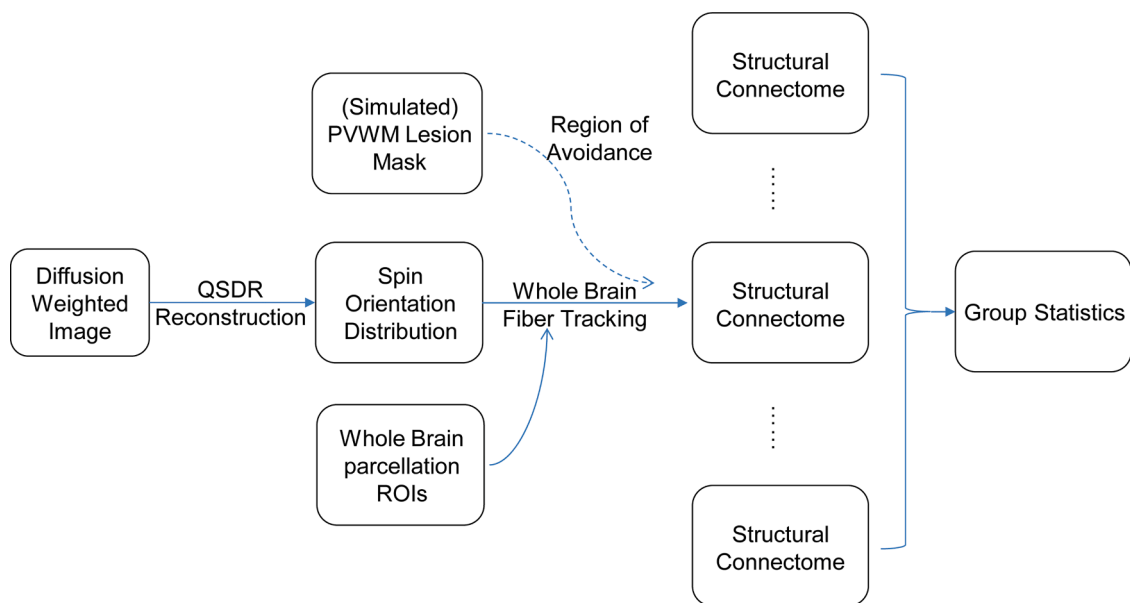


Fig. 1. Processing pipeline for the virtual lesion structural connectome.

The figure illustrates the workflow of the virtual lesion structural connectome calculation. The diffusion spin orientation distribution was first calculated from the diffusion weighted images using the q-space diffeomorphic reconstruction (QSDR) of DSI Studio [42]. Then whole brain fiber tracking was conducted on the spin orientation distribution using DSI Studio [42] with pre-defined whole brain parcellation ROIs. Optionally, during the whole brain fiber tracking, (simulated) PVWM ischemia masks were used as regions of avoidance to filter out DTI fibers passing through the lesion mask. After the fiber tracking, the structural connectomes of the subjects were collected for group statistical analysis to estimate the DTI disconnectome.

Additional validation of the predicted disconnectome using virtual lesions with simulated PVWM ischemia

We carried out two additional analyses to validate the methods and findings used this study. First, we compared the virtual lesion connectome obtained using a CBF-based ROA with that obtained using an ROA based on a WMH frequency map derived from the older cohort. Second, we leveraged the availability of both resting-state fMRI and DTI data in the older cohort to compare structural and functional connectivity changes using either HCP young subjects' DTI data or older subjects' native DTI data with or without lesion masks as ROA. These studies are described in the Supplement.

Results

White matter lesion frequency versus CBF mask

Fig. 2 compares WMH frequency in the $N = 46$ older subjects and cerebral blood flow (CBF) maps derived from arterial spin labeled perfusion MRI data in 436 middle aged subjects from the CARDIA study [33]. WMH are predominantly periventricular (Fig. 2A) and are encompassed within the boundaries of the relatively hypoperfused periventricular region (Fig. 2B).

Predicted disconnectome due to simulated PVWM ischemic lesions

Fig. 3 shows the network edges of the structural connectome derived from the $N = 30$ HCP young subjects datasets that were significantly reduced in strength with progressive PVWM ischemic lesion masks simulated using CBF data. Connections involving subcortical, cerebellar, and visual regions all show significant reductions in weight when compared to the full connectome. Connections with visual regions of interest (ROIs) and some subcortical ROIs were also affected, even with the smallest CBF masks (see red and orange grid points in Fig. 3). The full disconnectome matrix is shown in Supplemental Fig. S1.

Fig. 4A shows the average percentage of disconnected streamlines for the affected white matter tracts as a function of simulated progressive PVWM ischemic burden, sorted according to the CBF threshold for 50% disconnection. Optic radiations (OR), inferior fronto-occipital fasciculus (IFOF), inferior longitudinal fasciculus (ILF), corpus callosum (CC), temporopontine tract (TPT), and fornix were the pathways affected under the smallest simulated PVWM ischemic burden. Supplementary Fig. S2 shows the results for all 80 pathways. To better illustrate the evolution of affected WM fibers under simulated progressive PVWM ischemia, we generated a glass brain view of the affected WM fibers color-coded according to the lesion burden threshold for which they are affected (Fig. 4B) and a time-lapse animation of this evolution in Supplementary Video V1. The glass brain view also demonstrates that OR, IFOF, ILF, CC, and fornix were affected by low PVWM ischemic burdens (Fig. 4B).

Additional validations (see supplement)

Fig. S3 compares disconnectomes obtained using either the union of WMH lesion masks from the older cohort (Fig. S3A) or the group CBF map thresholded at $\text{CBF} \leq 16 \text{ ml}/100 \text{ g}/\text{min}$ (Fig. S3B) as ROAs. Fig. S3C shows the nodes corresponding to the disconnected edges for both ROA, demonstrating considerable overlap between approaches. We also assessed correlations between structural and functional connectivity across the older cohort, both using their native DTI data with or without WMH lesion masks as ROA and with indirect tractography using HCP young subjects' data. As shown in Fig. S6, correlations between structural and functional connectivity improved with WMH lesion masks as ROA and more substantially using indirect tractography with HCP young subjects' data. These results are described in greater detail in the Supplement.

Discussion

A virtual lesion approach was used along with indirect structural connectivity mapping to simulate the effects of progressive PVWM ischemia on both the structural connectome using cortical and subcortical parcellations as seed regions, and on WM pathways. Connectivity to parts of the visual system along with subcortical and cerebellar systems appeared most vulnerable to simulated early PVWM ischemic injury, while much more widespread involvement of both cortical and subcortical pathways was seen as simulated PVWM ischemic burden increased.

Even early PVWM ischemia was predicted to affect multiple pathways, likely reflecting the high density of crossing fibers in the periventricular regions as multiple white matter tracts skirt the ventricles. Pathways including optic radiations, inferior fronto-occipital fasciculus, inferior longitudinal fasciculus, corpus callosum, temporopontine tract and fornix were predicted to be affected. Early disruption of these pathways is consistent with previous literature suggesting that healthy aging is correlated with reduced integrity of inferior fronto-occipital fasciculus (associated with visual construction) and reduced integrity of inferior longitudinal fasciculus (associated with visuomotor dexterity and visual memory) [48,49]. Aging is also associated with degeneration of the corpus callosum [50,51] and optic radiations [51], the latter of which typically occur without visual field abnormalities [52]. Reduced fornix integrity has been associated with memory deficits and may predict conversion to cognitive impairment and dementia [53]. Rather than causing significant focal deficits, partial involvement of multiple pathways by PVWM ischemic injury may underlie the reductions in processing speed that characterize age-associated cognitive decline [6]. Although this study used high-resolution HCP DTI data, it remains possible that the full extent of disconnection due to PVWM ischemia was underestimated due to limitations in fiber tracking in the presence of crossing fibers.

Our finding of widespread partial disconnection due to PVWM ischemic lesions is also consistent with prior predictions based on healthy subject DTI data. Kuceyeski et al. used spherical synthetic lesions to map connectivity changes, including connectivity changes in frontal and parietal tracts associated with periventricular white matter [54]. Owen et al. used edge density mapping to predict that lesions in PVWM, and in particular posterior PVWM, would particularly disrupt brain connectivity [25]. Wang et al. then used Laplacian eigenmode decomposition of white matter diffusivity and found that periventricular white matter represented a key mode of overall brain connectivity [55].

In the current study, the ability to model the evolution of progressive PVWM ischemic injury using increasing CBF thresholds to identify vulnerable voxels allowed the predicted evolution of network disruption to be characterized. Note that the use of the CBF-based ROA also allowed connectivity effects of progressive PVWM ischemia to be predicted without contamination from DWM lesions that are also seen clinically with advancing age and subcortical ischemic lesion burden. Although WMH frequency maps could be edited to exclude DWM lesions, criteria for differentiating PVWM lesion and DWM lesions are empirical, whereas thresholding group CBF data provides a mechanistically based strategy. Another benefit of using CBF-based ischemic lesion masks derived from a middle aged cohort to simulate progressive PVWM ischemia lesions in a virtual lesion approach is that coregistration errors are expected to be minimally affected by significant atrophy that is typically present in older subjects.

An analogous virtual lesion approach can also be applied to WM lesion frequency maps available from large cohorts [3,5] as a complementary means of investigating the network consequences of hyperintensities seen on T2-weighted MRI, and this work is currently underway. The findings summarized in Fig. S3 suggest that connectivity changes would be very similar. Correlations between affected pathways and patterns of regional cortical atrophy can also contribute to understanding the mechanisms and network consequences of PVWM lesions

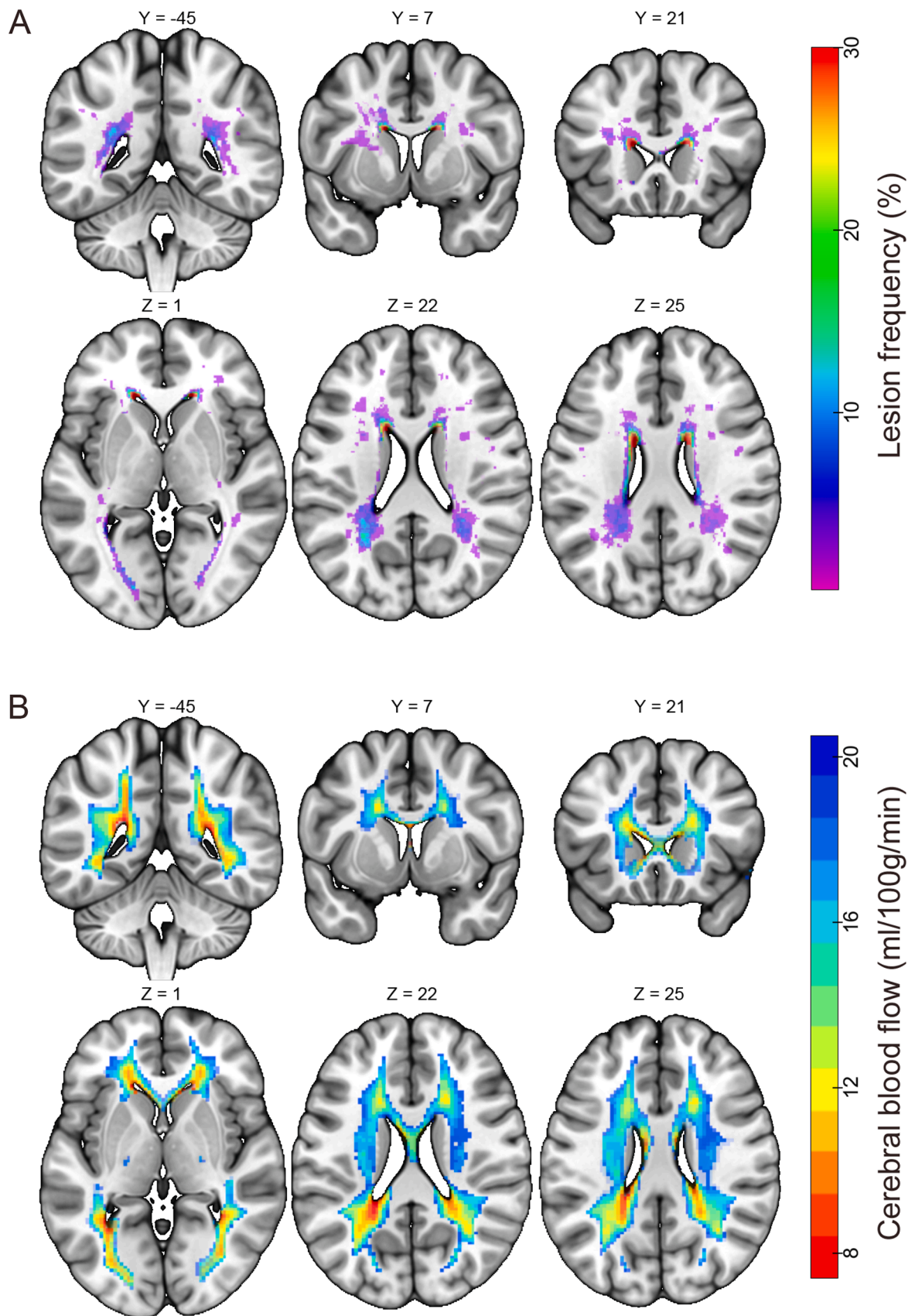


Fig. 2. White matter lesion frequency in subjects compared to cerebral blood flow in middle-aged subjects from [33].

(A) Voxel-wise white matter lesion frequency in the $N = 46$ older cohort, superimposed onto the Montreal Neurological Institute 152 standard space. (B) Group-averaged cerebral blood flow (CBF) map of $N = 436$ middle aged subjects [33] thresholded to show voxels with CBF in the 0–20 ml/100 g/min range, superimposed on the same brain slices as in panel (A).

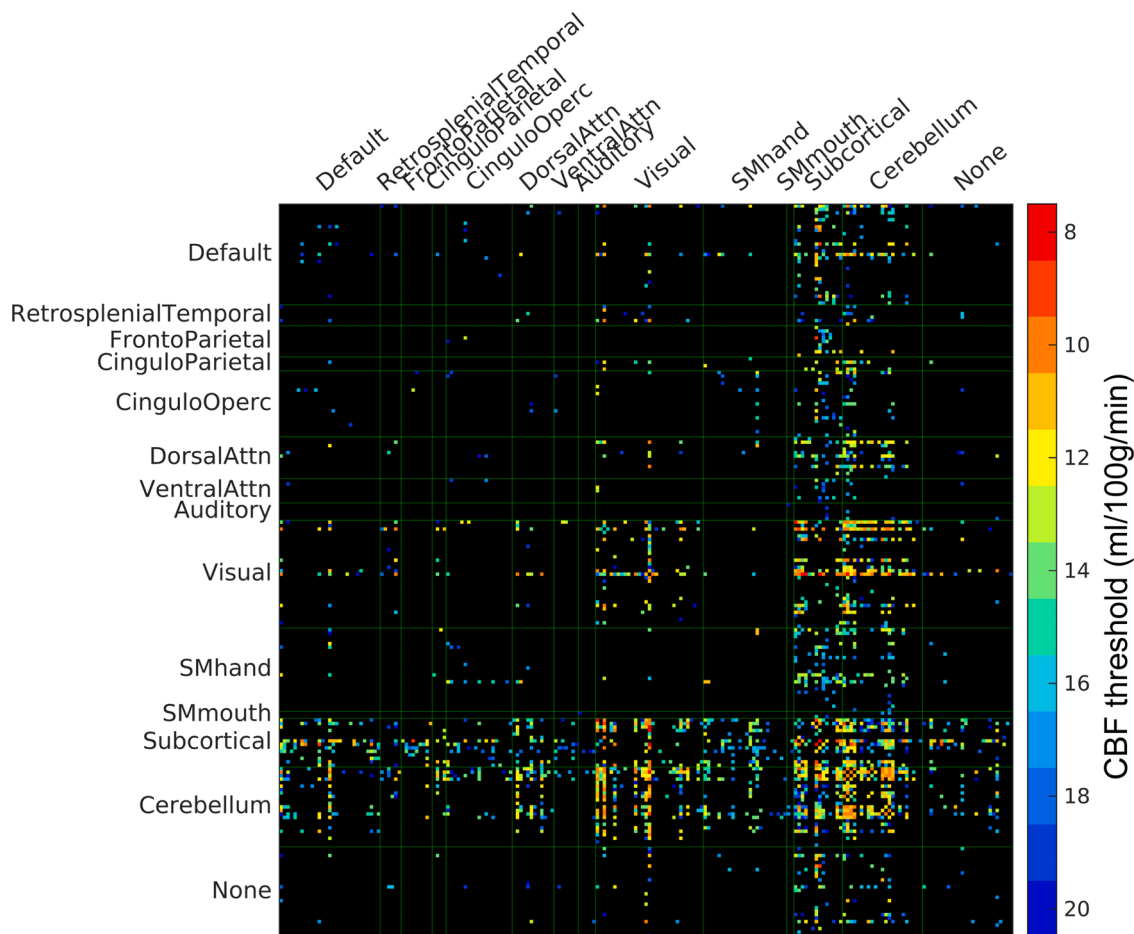


Fig. 3. PVWM disconnectome derived using CBF-based progressive PVWM ischemia simulation.

Edges with significant ($p < 0.05$, Bonferroni corrected) reduction of structural connectome are shown. The color scale shows the ROA mask CBF threshold at which significant disconnection was observed. For illustration purposes, the parcels with no edges of significant change have been eliminated in this matrix, the original full matrix can be found in supplementary Fig. S1. The nodes in the figure are grouped in brain cortical networks provided by Gordon et al. [40]: default mode (Default), retrosplenial temporal, frontoparietal, cingulo-parietal (CinguloParietal), cingulo-opercular (CinguloOperc), dorsal attention (DorsalAttn), ventral attention (VentralAttn), salience, auditory, visual, somatomotor hand (SMhand) and somatomotor mouth (SMmouth) networks and cortical regions not clustered to previous networks (None), as well as subcortical and cerebellum regions of AAL atlas [41] (For interpretation of the references to color in this figure, the reader is referred to the web version of this article).

by implicating Wallerian degeneration. Indeed, many of the ROIs affected in the virtual lesion based disconnectome, including calcarine, cuneus, insula, middle and superior frontal, lateral occipital, precentral and angular (Fig. S3C), have been associated with regional cortical atrophy in aging [56]. Recent work focusing on white matter voxel graphs for the purposes of connectome based lesion symptom mapping provides an alternative approach for rapidly estimating the effects of real or simulated PVWM ischemic lesions on cortex [57].

We showed that the virtual lesion approach improved correlations between structural connectivity and functional connectivity in a cohort of older subjects in whom both DTI and resting-state fMRI data were available. Virtual lesion structural connectivity calculated using indirect mapping with the older subjects' WM lesion masks as ROA and HCP young healthy subjects' DTI data showed a significantly higher correlation with the older subjects' functional connectivity than did direct mapping of the structural connectome using the older subjects' own DTI data. This finding supports the observation that the altered diffusion properties in the lesion area confounds fiber tracking algorithms [27, 28]. Applying older subjects' WM lesion masks as ROA during tractography on their own DTI data also improved the correlation with their functional connectivity, but to a much lesser extent than did the virtual lesion approach using HCP young subjects' DTI data. Since the latter approach requires coregistration between lesion masks derived from

older subjects and HCP DTI data acquired in healthy subjects, this finding also suggests that coregistration errors between WM lesion masks derived from older subjects and HCP DTI data from young subjects are not a major concern.

Because the disconnectomes generated here used regions of avoidance (ROA) in DTI tractography, the extent of true disconnection is likely overestimated. For example, the data shown in Fig. 4A suggest complete or nearly complete disconnection of at least parts of several pathways at higher simulated PVWM ischemic lesion burdens, whereas complete deficits such as visual field defects are not typically observed clinically [58]. Further, the maximum simulated ischemic lesion size of $\text{CBF} \leq 20 \text{ ml}/100 \text{ g}/\text{min}$ corresponds to an essentially complete lesion of the PVWM, which rarely occurs clinically. However, the majority of affected pathways do not show complete disconnection, particularly at lower CBF thresholds, and modeling partial rather than complete disconnection due to ROAs should only result in a scaling effect rather than any fundamental changes in the connectivity pattern, as has previously been demonstrated [55].

Since structure-function relationships between older subjects' functional connectivity data and structural connectivity derived from HCP healthy young subjects' DTI data even without any ROA were also stronger than when using older subjects' DTI data, some of the benefit of the virtual lesion approach seen might have been attributable to the

higher resolution of HCP DTI data and the increased accuracy (less noise) when using the averaged result of 30 HCP young subjects' DTI scan instead of each older subject's own single DTI scan. The recent availability of higher resolution DTI data from older subjects based on HCP protocols (HCP Lifespan data) may provide further understanding of differences between direct tractography and the indirect virtual lesion approach, as well as the impact of the age group from which healthy subject DTI data are derived. Moreover, functional connectivity does not necessarily reflect a single edge; therefore, changes in functional connectivity to compensate for structural connectivity deficits [59–61] may also serve to “normalize” overall functional connectivity. However, to the extent that correlations are expected between structural and functional connectivity, that the strongest correlations were observed when using the virtual lesion DTI approach supports the notion that virtual lesion DTI can be used to infer the effects of WM lesions on structural connectivity.

While the current study simulated the effects of progressive PVWM ischemia on the structural connectome using thresholded group CBF data, and an analogous approach could use WM lesion frequency maps as virtual lesions to evaluate structural connectivity changes due to white lesions more generally, the virtual lesion approach can also be applied to individual WM lesion masks to relate connectivity changes to cognitive performance in single subjects. If consistent relationships between tract disconnection and cognitive deficits can be established using either cross-sectional and/or longitudinal data, the individual subject disconnectome could ultimately be of value in the diagnosis of cognitive complaints, help disentangle the interactions between small vessel ischemic disease and neurodegeneration, and potentially guide neuro-modulatory strategies to reinforce the function of affected networks.

Conclusion

PVWM ischemic injury likely causes widespread partial disconnection. The optic radiations, inferior fronto-occipital fasciculus, inferior longitudinal fasciculus, corpus callosum, temporopontine tract and fornix are expected to be affected earliest in progressive PVWM ischemia, while the connectivity of subcortical, cerebellar, and visual regions is expected to be disrupted with increasing PVWM ischemic injury burden.

Declarations of Competing Interest

None.

Acknowledgement

This work was supported by NIH grants R21 AG070434, R01 NS111115, P30 AG010124, P41 EB015893, R03 AG063213, R01 AG055005, RF1 AG054409 and R01 HL127659. MH was supported in part by The Allen H. and Selma W. Berkman Charitable Trust (Accelerating Research on Vascular Dementia). DB was supported by The Paul G. Allen Family Foundation. DW was supported by the Diane Eisen Memorial Vascular Cognitive Impairment Research Fund. The HCP data were provided [in part] by the Human Connectome Project, WU-Minn Consortium (Principal Investigators: David Van Essen and Kamil Ugurbil; 1U54MH091657) funded by the 16 NIH Institutes and Centers that support the NIH Blueprint for Neuroscience Research; and by the McDonnell Center for Systems Neuroscience at Washington University. The funders had no role in study design, data collection and analysis, decision to publish, or preparation of the manuscript.

Supplementary materials

Supplementary material associated with this article can be found, in the online version, at [doi:10.1016/j.cccb.2021.100022](https://doi.org/10.1016/j.cccb.2021.100022).

References

- [1] N.D. Prins, P. Scheltens, White matter hyperintensities, cognitive impairment and dementia: an update, *Nat. Rev. Neurol.* 11 (3) (2015) 157–165.
- [2] M. Brant-Zawadzki, MR imaging of the aging brain: patchy white-matter lesions and dementia, *AJNR Am. J. Neuroradiol.* 6 (5) (1985) 675–682.
- [3] M. Habes, White matter lesions: spatial heterogeneity, links to risk factors, cognition, genetics, and atrophy, *Neurology* 91 (10) (2018) e964–e975.
- [4] C.M. Holland, Spatial distribution of white-matter hyperintensities in Alzheimer disease, cerebral amyloid angiopathy, and healthy aging, *Stroke* 39 (4) (2008) 1127–1133.
- [5] M. Habes, White matter hyperintensities and imaging patterns of brain ageing in the general population, *Brain* 139 (Pt 4) (2016) 1164–1179.
- [6] N.D. Prins, Cerebral small-vessel disease and decline in information processing speed, executive function and memory, *Brain* 128 (Pt 9) (2005) 2034–2041.
- [7] L. Griffanti, Classification and characterization of periventricular and deep white matter hyperintensities on MRI: a study in older adults, *Neuroimage* 170 (2018) 174–181.
- [8] M.S. Dharmoon, Periventricular white matter hyperintensities and functional decline, *J. Am. Geriatr. Soc.* 66 (1) (2018) 113–119.
- [9] J.T. O'Brien, H.S. Markus, Vascular risk factors and Alzheimer's disease, *BMC Med.* 12 (2014) 218.
- [10] R.N. Kalaria, M. Ihara, Dementia: vascular and neurodegenerative pathways-will they meet? *Nat. Rev. Neurol.* 9 (9) (2013) 487–488.
- [11] A.M. Brickman, Reconsidering harbingers of dementia: progression of parietal lobe white matter hyperintensities predicts Alzheimer's disease incidence, *Neurobiol. Aging* 36 (1) (2015) 27–32.
- [12] S.C. Larsson, H.S. Markus, Does treating vascular risk factors prevent dementia and Alzheimer's disease? A systematic review and meta-analysis, *J. Alzheimers Dis.* 64 (2) (2018) 657–668.
- [13] I.M. Nasrallah, White matter lesion penumbra shows abnormalities on structural and physiologic MRIs in the coronary artery risk development in young adults cohort, *AJNR Am. J. Neuroradiol.* 40 (8) (2019) 1291–1298.
- [14] N. Promjunyakul, Characterizing the white matter hyperintensity penumbra with cerebral blood flow measures, *Neuroimage Clin.* 8 (2015) 224–229.
- [15] P. Maillard, White matter hyperintensities and their penumbra lie along a continuum of injury in the aging brain, *Stroke* 45 (6) (2014) 1721–1726.
- [16] L. Pantoni, J.H. Garcia, Pathogenesis of leukoariosis: a review, *Stroke* 28 (3) (1997) 652–659.
- [17] K.W. Kim, J.R. MacFall, M.E. Payne, Classification of white matter lesions on magnetic resonance imaging in elderly persons, *Biol. Psychiatry* 64 (4) (2008) 273–280.
- [18] M.M. Reimer, Rapid disruption of axon-glia integrity in response to mild cerebral hypoperfusion, *J. Neurosci. Off. J. Soc. Neurosci.* 31 (49) (2011) 18185–18194.
- [19] E. Bullmore, O. Sporns, Complex brain networks: graph theoretical analysis of structural and functional systems, *Nat. Rev. Neurosci.* 10 (3) (2009) 186–198.
- [20] C.D. Langen, Disconnection due to white matter hyperintensities is associated with lower cognitive scores, *Neuroimage* 183 (2018) 745–756.
- [21] A.J. Lawrence, Structural network efficiency is associated with cognitive impairment in small-vessel disease, *Neurology* 83 (4) (2014) 304–311.
- [22] J. Tang, Aberrant white matter networks mediate cognitive impairment in patients with silent lacunar infarcts in basal ganglia territory, *J. Cereb. Blood Flow Metab.* 35 (9) (2015) 1426–1434.
- [23] A.M. Tuladhar, Structural network connectivity and cognition in cerebral small vessel disease, *Hum. Brain Mapp.* 37 (1) (2016) 300–310.
- [24] A.M. Tuladhar, Disruption of rich club organisation in cerebral small vessel disease, *Hum. Brain Mapp.* 38 (4) (2017) 1751–1766.
- [25] J.P. Owen, M.B. Wang, P. Mukherjee, Periventricular white matter is a nexus for network connectivity in the human brain, *Brain Connect.* 6 (7) (2016) 548–557.
- [26] J.M. Wardlaw, M.C. Valdés Hernández, S. Muñoz-Maniega, What are white matter hyperintensities made of? Relevance to vascular cognitive impairment, *J. Am. Heart Assoc.* 4 (6) (2015), 001140.
- [27] W. Reginold, Tractography at 3T MRI of corpus callosum tracts crossing white matter hyperintensities, *AJNR Am. J. Neuroradiol.* 37 (9) (2016) 1617–1622.
- [28] W. Reginold, Impact of white matter hyperintensities on surrounding white matter tracts, *Neuroradiology* 60 (9) (2018) 933–944.
- [29] S. Muñoz Maniega, Spatial gradient of microstructural changes in normal-appearing white matter in tracts affected by white matter hyperintensities in older age, *Front Neurol.* 10 (2019) 784.
- [30] S. Seiler, Cerebral tract integrity relates to white matter hyperintensities, cortex volume, and cognition, *Neurobiol. Aging* 72 (2018) 14–22.
- [31] J. Gomez, Functionally defined white matter reveals segregated pathways in human ventral temporal cortex associated with category-specific processing, *Neuron* 85 (1) (2015) 216–227.
- [32] A. Salvaggio, Post-stroke deficit prediction from lesion and indirect structural and functional disconnection, *Brain* 143 (7) (2020) 2173–2188.
- [33] S. Dolui, Characterizing a perfusion-based periventricular small vessel region of interest, *Neuroimage Clin.* 23 (2019), 101897.
- [34] P. Maillard, Coevolution of white matter hyperintensities and cognition in the elderly, *Neurology* 79 (5) (2012) 442–448.
- [35] P. Maillard, White matter hyperintensity penumbra, *Stroke* 42 (7) (2011) 1917–1922.
- [36] N.O. Promjunyakul, Baseline NAWM structural integrity and CBF predict periventricular WMH expansion over time, *Neurology* 90 (24) (2018) e2119–e2126.

- [37] D.C. Van Essen, The WU-minn human connectome Project: an overview, *Neuroimage* 80 (2013) 62–79.
- [38] S.N. Sotiropoulos, Advances in diffusion MRI acquisition and processing in the human connectome project, *Neuroimage* 80 (2013) 125–143.
- [39] P. Schmidt, An automated tool for detection of FLAIR-hyperintense white-matter lesions in multiple sclerosis, *Neuroimage* 59 (4) (2012) 3774–3783.
- [40] E.M. Gordon, Generation and evaluation of a cortical area parcellation from resting-state correlations, *Cereb. Cortex* 26 (1) (2016) 288–303.
- [41] E. Mellet, Neural basis of mental scanning of a topographic representation built from a text, *Cereb. Cortex* 12 (12) (2002) 1322–1330.
- [42] F.C. Yeh, V.J. Wedeen, W.Y. Tseng, Estimation of fiber orientation and spin density distribution by diffusion deconvolution, *Neuroimage* 55 (3) (2011) 1054–1062.
- [43] E. van Dellen, Minimum spanning tree analysis of the human connectome, *Hum. Brain Mapp.* 39 (6) (2018) 2455–2471.
- [44] J.A. Roberts, Consistency-based thresholding of the human connectome, *Neuroimage* 145 (Pt A) (2017) 118–129.
- [45] J.D. Power, Functional network organization of the human brain, *Neuron* 72 (4) (2011) 665–678.
- [46] F.C. Yeh, Population-averaged atlas of the macroscale human structural connectome and its network topology, *Neuroimage* 178 (2018) 57–68.
- [47] F.C. Yeh, W.Y. Tseng, NTU-90: a high angular resolution brain atlas constructed by q-space diffeomorphic reconstruction, *Neuroimage* 58 (1) (2011) 91–99.
- [48] A.N. Voineskos, Age-related decline in white matter tract integrity and cognitive performance: a DTI tractography and structural equation modeling study, *Neurobiol. Aging* 33 (1) (2012) 21–34.
- [49] N. Shinoura, Impairment of inferior longitudinal fasciculus plays a role in visual memory disturbance, *Neurocase* 13 (2) (2007) 127–130.
- [50] M. Ota, Age-related degeneration of corpus callosum measured with diffusion tensor imaging, *Neuroimage* 31 (4) (2006) 1445–1452.
- [51] A. Peters, The effects of normal aging on myelin and nerve fibers: a review, *J. Neurocytol.* 31 (8–9) (2002) 581–593.
- [52] M. Kitajima, Hyperintensities of the optic radiation on T2-weighted MR images of elderly subjects, *AJNR Am. J. Neuroradiol.* 20 (6) (1999) 1009–1014.
- [53] V. Douet, L. Chang, Fornix as an imaging marker for episodic memory deficits in healthy aging and in various neurological disorders, *Front Aging Neurosci.* 6 (2014) 343.
- [54] A. Kuceyeski, The generation and validation of white matter connectivity importance maps, *Neuroimage* 58 (1) (2011) 109–121.
- [55] M.B. Wang, Brain network eigenmodes provide a robust and compact representation of the structural connectome in health and disease, *PLoS Comput. Biol.* 13 (6) (2017), e1005550.
- [56] A. Bakkour, The effects of aging and Alzheimer’s disease on cerebral cortical anatomy: specificity and differential relationships with cognition, *Neuroimage* 76 (2013) 332–344.
- [57] C. Greene, Finding maximally disconnected subnetworks with shortest path tractography, *Neuroimage Clin.* 23 (2019), 101903.
- [58] D. Pascolini, S.P. Mariotti, Global estimates of visual impairment: 2010, *Br. J. Ophthalmol.* 96 (5) (2012) 614–618.
- [59] D. Barulli, Y. Stern, Efficiency, capacity, compensation, maintenance, plasticity: emerging concepts in cognitive reserve, *Trends Cogn. Sci.* 17 (10) (2013) 502–509 (Regul. Ed.).
- [60] A. Celegghin, Intact hemisphere and corpus callosum compensate for visuomotor functions after early visual cortex damage, *Proc. Natl. Acad. Sci. U. S. A.* 114 (48) (2017). E10475-E10483.
- [61] A. Iraj, Compensation through functional hyperconnectivity: a longitudinal connectome assessment of mild traumatic brain injury, *Neural Plast.* (2016), 4072402, 2016.